PHYSICAL REVIEW D VOLUME 29, NUMBER 11 1 JUNE 1984

Direct photon production at CERN ISR, CERN collider, and Fermilab Tevatron energies

E. N. Argyres
State University College, Plattsburgh, New York 12901

A. P. Contogouris, M. Sanielevici, and H. Tanaka
Department of Physics, McGill University, Montreal, Canada H3A 2T8
(Received 17 January 1984)

Predictions are presented for large-p_T direct photon production in $\bar{p}p$ collisions at CERN ISR ($\sqrt{s}=63$ GeV), CERN collider (540 GeV), and Fermilab Tevatron (1600 GeV) energies in perturbative QCD. Two sets of gluon and other parton distributions determined from deep-inelastic scattering are used. Higher-order corrections (K factors) are approximately taken into account. Contributions from photon bremsstrahlung graphs and the related fractions of photon events accompanied by hadrons are presented and discussed in detail.

I. INTRODUCTION

Direct photon production in hadronic collisions at large transverse momentum (p_T) has been an important test of perturbative QCD (PQCD).[1-4]

With the successful operation of the CERN collider, one anticipates that direct γ data will soon be available at much higher energy ($\sqrt{s}=540$ GeV). In fact, proposals for such collider experiments have already been submitted.[5] It is therefore important to present detailed theoretical predictions at such s.

On the other hand, two experiments are underway for large-p_T $\bar{p}p\to\gamma+X$ at the CERN ISR, and results are expected to become available soon.[6] PQCD has been successful for $pp\to\gamma+X$ at the ISR;[1,2,4] it is clearly important to confront its predictions with data on $\bar{p}p\to\gamma+X$ as well, thus covering a large range of values of $\sqrt{s}$.

Finally we present predictions for $\bar{p}p\to\gamma+X$ at $\sqrt{s}=1600$ GeV (Fermilab Tevatron).

For one reason, particular interest in direct γ production arises from the fact that it provides important tests or constraints on the gluon distribution. Analyses of deep-inelastic neutrino data have now produced detailed forms of the gluon distribution in the nucleon, and in fact detailed sets of parton distributions.[7,8] It is of interest to see to what extent these distributions will be successful in describing the ISR and in particular the collider and Tevatron $\bar{p}p\to\gamma+X$ data.

The first collider data are expected to cover the range $4\lesssim p_T\lesssim 10$ GeV.[5] The corresponding values of $x_T\equiv 2p_T/\sqrt{s}$ ($1.5\times10^{-2}\lesssim x_T\lesssim 3.7\times10^{-2}$) are quite small. At such small x the usual QCD determinations and the parametrizations of the parton distributions (particularly of the gluon), including their Q^2 dependence,[7,8] are subject to serious uncertainties. We present detailed predictions using two different sets of parton distributions,[7,8] and we hope that we thus give an idea of the magnitude of the uncertainties involved in such a theoretical calculation (this point is further discussed in Sec. V, in relation with confronting PQCD predictions with low-x_T collider data on $\bar{p}p\to\pi+X$). Similar remarks hold for our Tevatron predictions at the lower p_T.

In the past there has been some interest regarding bremsstrahlung (brems) contributions to large-p_T γ production, i.e., from the subprocesses $qq\to qq\gamma$, $qg\to qg\gamma$, etc.[9-14] We present detailed predictions for brems contributions as well. One reason for a particular interest is the following. As we discuss in Sec. II, the dominant part of such contributions is believed to correspond to the final photon being collinear with one of the final partons. Since the final partons materialize in hadron jets, in most of the brems events the large-p_T photon is accompanied by hadrons. This is in contrast with events arising from the basic QCD subprocesses [Eqs. (2.1) and (2.2) below], where the photon is unaccompanied. Some of the proposed experiments[5] are expected to provide information on accompanied vs unaccompanied photons, thus disentangling, to some extent, the various QCD mechanisms.

Finally, in recent years there has been much work on large corrections from higher-order PQCD contributions (K factors). We take such corrections into account in a rough approximation. As we discuss, their size is comparable to that of other theoretical uncertainties (e.g., the form of the gluon distribution or the choice of the large variable Q^2). Thus the main purpose for presenting results with our K factors is to also give an idea of the magnitude of the theoretical uncertainties regarding the effects of higher-order corrections.

Section II presents the basic formulas we use for the fundamental QCD subprocesses and the brems contributions. Section III deals with the input information and the uncertainties related with it and with the choice of the certain variables. Section IV discusses the K factors. Section V presents our results and discusses several of their aspects. Finally, Sec. VI discusses some aspects of the brems contributions and of our predictions regarding accompanied vs unaccompanied photons.

II. BASIC FORMULAS

QCD studies of direct γ production are based on the subprocesses

$$q+g\to q+\gamma\ , \tag{2.1}$$

$$q+\bar{q}\to g+\gamma\ . \tag{2.2}$$

Their lowest-order differential cross sections [Born, of $O(\alpha_s)$] to be denoted by $d\sigma_0/d\hat{t}$ are well known,[15,16] they are reproduced here for completeness:

$$\frac{d\sigma_0}{d\hat{t}}(qg)=e_q{}^2\frac{\pi\alpha\alpha_s}{3\hat{s}^2}\frac{\hat{s}^2+\hat{t}^2}{-\hat{t}\hat{s}}\ , \tag{2.3}$$

$$\frac{d\sigma_0}{d\hat{t}}(q\bar{q})=e_q{}^2\frac{8\pi\alpha\alpha_s}{9\hat{s}^2}\frac{\hat{t}^2+\hat{u}^2}{\hat{t}\hat{u}}\ , \tag{2.4}$$

where $\hat{s}$, $\hat{t}$, $\hat{u}$ are the subprocess Mandelstam variables. In this work we consider γ production at $\theta=90°$ in the c.m. of the colliding hadrons. Then the contribution of the subprocess $a+b\to c+\gamma$ to the inclusive cross section for $A+B\to\gamma+X$ is

$$E\frac{d\sigma_0}{d^3p}(p_T,s)=\frac{2}{\pi}\int_{x_1}^1\frac{dx_a}{2x_a-x_T}F_{a/A}(x_a,Q^2)\times F_{b/B}(x_b,Q^2)\frac{d\sigma_0}{d\hat{t}}+(A\leftrightarrow B)\ , \tag{2.5}$$

where $F_{a/A}$ denotes momentum distribution, etc., $x_T=2p_T/\sqrt{s}$ and

$$x_b=x_T\frac{x_a}{2x_a-x_T},\quad x_1=\frac{x_T}{2-x_T}\ . \tag{2.6}$$

Photons at large p_T may also arise via brems, i.e., from subprocesses of the type $a+b\to c+d+\gamma$. Typical cases are

$$q+q\to q+q+\gamma\ , \tag{2.7}$$

$$q+g\to q+g+\gamma\ , \tag{2.8}$$

$$g+g\to q+\bar{q}+\gamma\ . \tag{2.9}$$

The contribution of Eq. (2.7) has been calculated completely to $O(\alpha_s{}^2)$. Then it was found that its dominant part arises from the kinematic configurations in which the γ is produced collinearly with one of the final quarks. This part corresponds to $qq\to qq$ with a subsequent fragmentation $q\to\gamma$; the fragmentation function is proportional to $\ln Q^2$ (see below). The remaining part ("constant piece") is very small throughout the entire kinematic range.[9-11] We anticipate a similar situation for all brems-type subprocesses, and subsequently calculate the dominant part for all of them. Then the contribution of $a+b\to c+d+\gamma$ to $A+B\to\gamma+X$ is

$$E\frac{d\sigma_0}{d^3p}(p_T,s,\theta)=\frac{1}{\pi}\int_{x_1}^1\frac{dx_a}{x_a}\int_{x_2}^1\frac{dx_b}{x_b}F_{a/A}(x_a,Q^2)F_{b/B}(x_b,Q^2)\times\frac{d\tilde{\sigma}_0}{d\hat{t}}D_{\gamma/c}(z,Q^2)\frac{1}{z^2}+(A\leftrightarrow B)\ . \tag{2.10}$$

Here $d\tilde{\sigma}_0/d\hat{t}$ is the Born [of $O(\alpha_s{}^2)$] differential cross section for $a+b\to c+d$, $D_{\gamma/c}$ the fragmentation function $c\to\gamma$ (momentum distribution), and for $\theta=90°$, x_1 is given by Eq. (2.6), and

$$x_2=x_T\frac{x_a}{2-x_T},\quad z=\frac{x_T}{2}\left[\frac{1}{x_a}+\frac{1}{x_b}\right], \tag{2.11}$$

The fragmentation function is of the form

$$D_{\gamma/c}(z,Q^2)=\frac{\alpha}{2\pi}d_{\gamma/c}(z)\ln\frac{Q^2}{\tilde{\Lambda}^2}\ , \tag{2.12}$$

where $\tilde{\Lambda}$ is some scale. To the lowest nontrivial order[9-11]

$$d_{\gamma/q}(z)=e_q{}^2[1+(1-z)^2]\ . \tag{2.13}$$

There has been much work regarding $D_{\gamma/c}(z,Q^2)$ [and the structure functions $F_{c/\gamma}(z,Q^2)$] by summing leading-logarithmic contributions. Then one obtains the simple form[17]

$$d_{\gamma/q}(z)=\frac{1.124z}{1-0.72\ln(1-z)}\ . \tag{2.14}$$

This has the right behavior at $z\sim1$, but for smaller z it significantly deviates from the exact result.[18] A better parametrization is provided by the forms[18]

$$d_{\gamma/q}(z)=2z^{-0.6}\sum_{n=0}^{4}a_nz^n\ , \tag{2.15}$$

where for $e_q{}^2=\frac{4}{9}$,

$$a_0=0.025,\ a_1=0.87,\ a_2=-2.63\ ,\quad a_3=3.34,\ a_4=-1.546\ , \tag{2.16}$$

and for $e_q{}^2=\frac{1}{9}$,

$$a_0=0.014,\ a_1=0.15,\ a_2=-0.457\ ,\quad a_3=0.577,\ a_4=-0.272\ . \tag{2.17}$$

We use the forms (2.15), but we also present certain results with, and we comment on, the forms (2.14) and (2.13).

To the lowest nontrivial order a gluon cannot fragment to a photon [$d_{\gamma/g}(z)=0$, corresponding to Eq. (2.13)]. In the leading-logarithmic approximation, however, due to transitions $g\to q\bar{q}$ with subsequent fragmentation $q\to\gamma$ (or $\bar{q}\to\gamma$), $d_{\gamma/g}(z)\neq0$. We shall present results for the subprocesses $gg\to gg\gamma$ and $qg\to qg\gamma$ (with $g\to\gamma$) using $d_{\gamma/g}(z)$ of the form (2.15) with[18]

$$a_0=0.021,\ a_1=-0.03,\ a_2=-0.0057\ ,\quad a_3=0.03,\ a_4=-0.015\ . \tag{2.18}$$

III. INPUT INFORMATION AND UNCERTAINTIES

To give a measure of the uncertainties involved regarding the input distributions $F_{a/A}$ (mainly the gluon distribution), we present predictions with two different sets. This is particularly important for collider (and Tevatron)

experiments, where at least the first data will correspond to relatively low p_T, thus very small x_T.

(I) The first set (subsequently denoted CDHS) is the complete set of Ref. 7 including their Q^2 dependence (scale violations). In this the gluon distribution has the form

$$F_{g/p}(x,Q_0{}^2=5\ \mathrm{GeV}^2)=2.616(1+3.5x)(1-x)^{5.9}\ . \quad (3.1)$$

(II) The second set (to be denoted GHR) is the complete set of Ref. 8 (including scale violations). In this

$$F_{g/p}(x,Q_0{}^2=4\mathrm{GeV}^2)$$
$$=0.93(1+8.5x+53.57x^2)(1-x)^6\ . \quad (3.2)$$

This form, in the determination of which charm-threshold effects are taken into account,[8] is somewhat broader than Eq. (3.1). Both sets CDHS and GHR are determined from analyses of deep-inelastic-scattering structure-function data.

Additional uncertainties in our predictions arise from the choice of the "large" variable Q^2, of the scale Λ in the running coupling constant $\alpha_s(Q^2)=12\pi/25\ln(Q^2/\Lambda^2)$ and of $\tilde{\Lambda}$ in Eq. (2.12). We use

$$Q^2=2p_T{}^2 \quad (3.3)$$

on account of the fact that with this choice the resulting scale violations are known to be intermediate;[16] and we comment on other choices. Also we use[7]

$$\Lambda=\tilde{\Lambda}=0.2\ \mathrm{GeV}\ . \quad (3.4)$$

At ISR energies, effects due to partons' intrinsic transverse momentum, (k_T) are not very important for direct γ production (see Ref. 10 for a detailed calculation); they are even less important at the collider at Tevatron, where as a function of p_T, the cross section is less steep. Nevertheless, we take them into account assuming partons on-shell and a Gaussian distribution with modest

$$\langle k_T\rangle=0.5\ \mathrm{GeV}\ . \quad (3.5)$$

Finally, for the cross sections $d\tilde{\sigma}_0/d\hat{t}$ in Eq. (2.10) we use the results of Ref. 19, without any change.

IV. K FACTORS

Higher-order QCD perturbative corrections are known to modify the Born cross sections, usually by some factor (K factor) which is almost constant over a wide kinematic range. Such corrections arise from loop graphs (with virtual gluons) and gluon brems. In several cases, notably in Drell-Yan dilepton production, such K factors seem to be required by experiment.

References 10 and 16 used a strong gluon distribution of the form

$$F_{g/p}(x,Q_0{}^2=4\ \mathrm{GeV}^2)=0.866(1+9x)(1-x)^4\ ;$$

this is stronger than Eq. (3.1) and for $x\lesssim 0.5$ about as strong as Eq. (3.2) [for $x\gtrsim 0.5$ it is stronger than both Eqs. (3.1) and (3.2)]. Reference 10 took also into account the complete brems contribution of the subprocess (2.7). Still it was found that ISR $pp\to\gamma+X$ data required a K factor, roughly $K\sim 2$.[20,1,4]

For the subprocesses (2.1) and (2.2), which are essential in the QCD treatment of large-p_T γ production, no complete calculation of the higher-order corrections is yet available.[20a] The same is true for all the subprocesses $ab\to cd$ leading to the brems contributions [Eq. (2.10)] (with the exception of $qq'\to qq'$, nonidentical quarks, where complete calculations give $K\sim 2.5$). Such calculations are quite lengthy, and final results are very complicated and often untransparent.

Nevertheless, for several large transfer processes, π^2 terms similar to those of Drell-Yan dilepton production (arising from loop graphs in the soft-gluon limit), as well as certain collinear gluon brems configurations, have led to a correct estimate of the bulk of the correction.[20–22] In particular, for the subprocess (2.1), which dominates large-p_T $pp\to\gamma+X$, the techniques of Ref. 20 have led to a K factor which significantly improves agreement with experiment (see also below). Also for the subprocess $q\bar{q}\to\gamma^* g$, which is closely related with Eq. (2.2) (and is important in large-p_T $\pi^- N\to l^+l^-+X$ and $\bar{p}N\to l^+l^-+X$), a K factor has been determined again in agreement with the data as well as with complete theoretical calculations.[22,23]

Thus for Eqs. (2.1) and (2.2) we proceed with the results of Refs. 20 and 22. To $O(\alpha_s{}^2)$ these amount to subprocess cross sections of the form

$$\frac{d\sigma}{d\hat{t}}\simeq K\frac{d\sigma_0}{d\hat{t}},\quad K\simeq 1+\frac{\alpha_s(Q^2)}{2\pi}C\pi^2\ , \quad (4.1)$$

where C is a color factor; in particular,

$$C(qg\to q\gamma)=N_c-C_F,\quad C(q\bar{q}\to g\gamma)=C_F \quad (4.2)$$

with $N_c=3$ and $C_F=\frac{4}{3}$ in color SU(3). Note that Eqs. (4.2) imply comparable corrections to Eqs. (2.1) and (2.2).[24]

For the subprocesses $ab\to cd$ of the brems contributions the techniques of Refs. 20–22 have also been applied and led to a set of K factors similar to those in Eq. (4.1).[25] We shall use the results of Ref. 25 as an indication (rough estimate) of the possible effects of higher-order QCD corrections to the brems contributions.

V. RESULTS AND DISCUSSION

First of all as a test of the input distributions (CDHS and GHR) and of our overall approach we first carry a calculation for $pp\to\gamma+X$ at $\sqrt{s}=63$ GeV and compare it with available data.[26] The results are presented in Fig. 1. On the whole, agreement with the data is very satisfactory, except, perhaps, at low p_T ($\lesssim 5$ GeV); in this region agreement could be improved (if necessary) by choosing a larger $\langle k_T\rangle$. Notice that, at least with the CDHS distributions (solid curves), inclusion of our K factors improves the overall agreement.

To compare direct γ with π^0 yields we introduce as usual the ratio

$$\left[\frac{\gamma}{\pi^0}\right]_{AB}\equiv\frac{E\,d\sigma(AB\to\gamma X)/d^3p}{E\,d\sigma(AB\to\pi^0X)/d^3p}\ . \quad (5.1)$$

Regarding $AB\to\pi^0X$, throughout this work we try to use experimental data as much as possible. For $pp\to\pi^0+X$

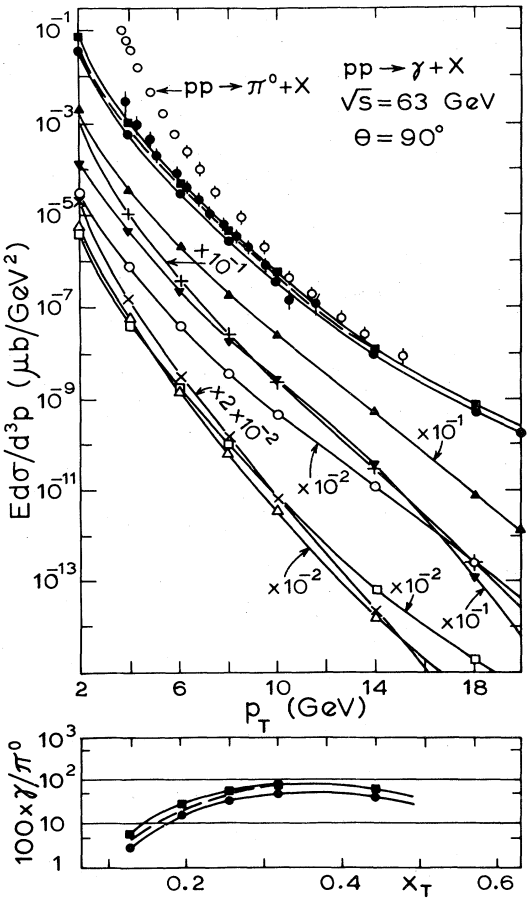

FIG. 1. $pp \to \gamma + X$ at ISR energy. All solid curves correspond to calculations using the CDHS set: —●— sum of Born contributions [$O(\alpha_s)$ and brems]; —■— including K factors and k_T effects; —▲— contribution of $qg \to q\gamma$ [Eq. (2.1)] divided by 10; —▼— $q\bar{q} \to g\gamma$ [Eq. (2.2)] divided by 10; —+— $qg \to qg\gamma$ (with $q \to \gamma$) divided by 10; —○— $qq \to qq\gamma$ (multiplied by 10^{-2}); —△— $gg \to q\bar{q}\gamma$ (multiplied by 10^{-2}); —×— $gg \to gg\gamma$ (multiplied by 2×10^{-2}); —□— $qg \to qg\gamma$ (with $g \to \gamma$) (multiplied by 10^{-2}). Dashed curve: sum of Born contributions [$O(\alpha_s)$ and brems] using the GHR set. Experimental data: ♦ $pp \to \gamma + X$ (Ref. 26), ○ $pp \to \pi^0 + X$ (Ref. 26). The lower part ($100\times\gamma/\pi^0$) is determined by dividing the corresponding curves of the upper part by an interpolation through the $pp \to \pi^0 + X$ data.

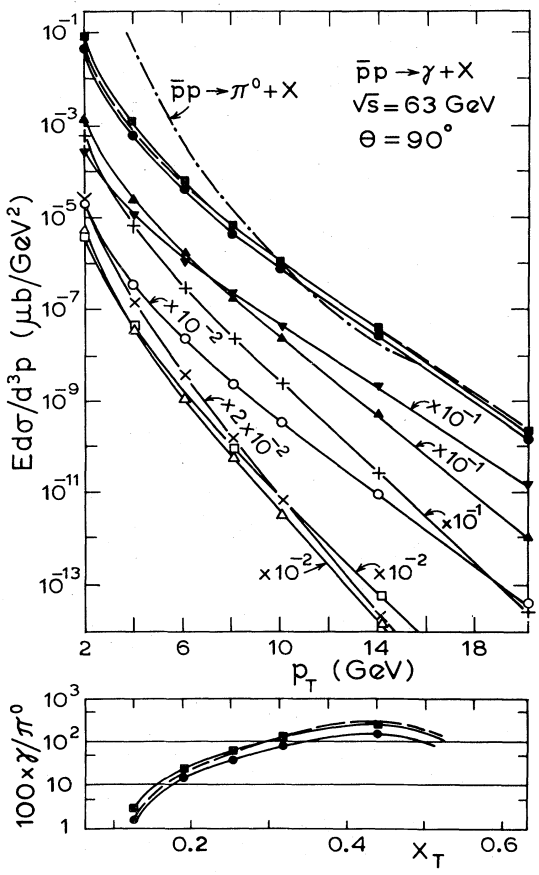

FIG. 2. $\bar{p}p \to \gamma + X$ at ISR energy. Solid and dashed curves as in Fig. 1. Dash-dotted curve: corresponding to $\bar{p}p \to \pi^0 + X$ (see text). The lower part is determined as in Fig. 1.

such data are available in detail,[26] and we use an interpolation through them in order to form $(\gamma/\pi^0)_{pp}$ (Fig. 1, lower part).

For $pp \to \gamma + X$ and $(\gamma/\pi^0)_{pp}$ several calculations have already been presented, e.g., in Ref. 10 (without K factors) and in Ref. 20 (with K factors). Although the present calculations differ in several respects (use of more recent parton distributions, inclusion of more brems subprocesses, etc.), it can be said that the present results are not far from those obtained in Refs. 10 and 20 with a strong gluon distribution.

Next we turn to $\bar{p}p \to \gamma + X$ at ISR ($\sqrt{s} = 63$ GeV); our results are shown in Fig. 2.

A point to notice is that at low p_T ($\lesssim 4$ GeV) $\bar{p}p \to \gamma + X$ is only slightly above $pp \to \gamma + X$, but as p_T increases, the former exceeds the latter more and more. This is essentially because $\bar{p}$ contains valence antiquarks, so as p_T increases (x_T increases), the contribution of subprocesses Eq. (2.2) becomes more and more important. Regarding the ratio

$$r \equiv \frac{E\, d\sigma(\bar{p}p \to \gamma X)/d^3p}{E\, d\sigma(pp \to \gamma X)/d^3p}\,, \tag{5.2}$$

we predict the following: At $p_T = 6$ GeV, $r \simeq 1.4$ with both CDHS and GHR distributions; at $p_T = 8$ GeV, $r = 1.7$ with CDHS and $r = 1.64$ with GHR. Notice the stability of r against CDHS vs GHR. We found similar values for r by changing the large variable from $Q^2 = 2p_T{}^2$ to $Q^2 = p_T{}^2$, or by changing Λ. It can be said that r is quite stable against various uncertainties of our calculation, and this is understandable since it mainly depends on the increasing importance of the subprocess (2.2) in $\bar{p}p \to \gamma + X$.

Figure 2, lower part, presents $(\gamma/\pi^0)_{\bar{p}p}$. For $\bar{p}p \to \pi^0 + X$ we use the indicated cross section (dash-dotted curve of upper part); this is taken to be the same as $pp \to \pi^0 + X$ (Fig. 1), as is supported by recent data[27] and by theoretical calculations.[25] We predict $(\gamma/\pi^0)_{\bar{p}p} \simeq 1$ at $p_T \simeq 9-10$ GeV, depending on whether we use GHR or

CDHS distributions. At higher p_T, $(\gamma/\pi^0)_{\bar{p}p}$ is predicted to significantly exceed 1.

Now we consider $\bar{p}p \to \gamma + X$ at the collider, and present our results in Fig. 3. As in Figs. 1 and 2, solid squares (upper curve) correspond to the sum of all contributions with K factors and k_T effects calculated with CDHS distributions; solid circles to the sum of the corresponding Born terms (with CDHS); and the dashed curve is the sum of Born contributions with GHR.

Regarding $\bar{p}p \to \pi^0 + X$ in the ratio $(\gamma/\pi^0)_{\bar{p}p}$ we proceed as follows. For $p_T \lesssim 4.5$ GeV we interpolate through available data;[28] for $p_T > 4.5$ GeV, we use the theoretical calculation of Ref. 25 with the overall normalization slightly adjusted to fit the data well at $p_T \lesssim 4.5$ GeV. Anyway, our $E\,d\sigma(\bar{p}p \to \pi^0 X)/d^3p$ is also shown in Fig. 3, upper part. Then Fig. 3, lower part, shows our predictions for $(\gamma/\pi^0)_{\bar{p}p}$. With CDHS distributions we predict $(\gamma/\pi^0)_{\bar{p}p} \simeq 1$ at $p_T \simeq 50$ GeV; with GHR at $p_T \simeq 40$ GeV. It is significant that Ref. 29 has a similar prediction although it uses a different set of parton distributions,

$$F_{g/p}(x, Q_0^2 = 1.8\ \text{GeV}^2) \sim (1-x)^5 .$$

In the range $15 \lesssim p_T \lesssim 30$ GeV there are some preliminary data for $\bar{p}p \to$ neutral $+ X$, where neutral $= \gamma$, π^0, or η.[30] Regarding γ they can be summarized by stating

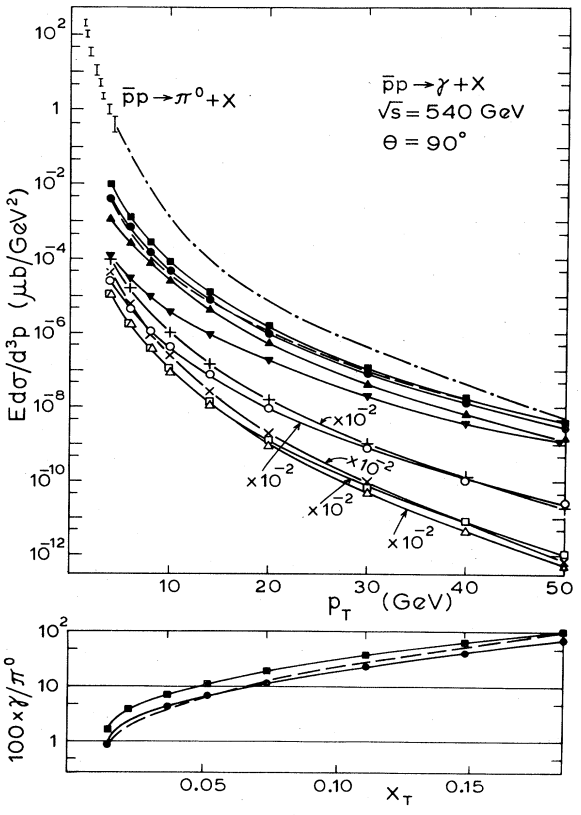

FIG. 3. $\bar{p}p \to \gamma + X$ at the collider. Solid and dashed curves as in Fig. 1, but with multiplication factors as indicated. Dash-dotted curve: corresponding to $\bar{p}p \to \pi^0 + X$ (see text). The lower part is determined as in Fig. 1.

$(\gamma/\text{jet})_{\bar{p}p} \lesssim 10^{-3}$. Our predictions are consistent with this result.

Note that in the entire p_T range of Fig. 3 the contribution of the subprocess Eq. (2.1) exceeds that of (2.2). The same is true in $\bar{p}p \to \gamma + X$ at $\sqrt{s} = 63$ GeV (Fig. 2) for $p_T \lesssim 7$. The reason is that the corresponding $x_T (\lesssim 0.2)$ is small, so that $F_{g/p}(x, Q^2)$ is bigger than $F_{q/p}(x, Q^2)$.[7,8] Of course, as x_T increases, the subprocess (2.2) becomes more and more important.

As we discussed in the Introduction, at the lower p_T the corresponding x_T at the collider are very small and, in principle, our predictions are subject to serious uncertainties. Notice, however, that the CDHS and GHR predictions (solid circles vs dashed curves, both total Born) differ little (at $x_T \lesssim 0.1$). Perhaps this indicates that our predictions are not completely untrustworthy. Furthermore, for $\bar{p}p \to \pi^0 + X$, Ref. 25 obtained good agreement with collider data down to $p_T = 2 (x_T \simeq 7.5 \cdot 10^{-3})$ with both the CDHS and GHR set. In general π^0 production is more complicated than direct photon production (presence of fragmentation functions, greater importance of $\langle k_T \rangle$, etc). Thus we see no reason to completely distrust our results at the lower p_T.

At a fixed p_T, the predicted direct γ yields at the collider are significantly higher than those at ISR. As an example, consider $p_T = 10$ GeV. With CDHS, $\bar{p}p \to \gamma + X$ at $\sqrt{s} = 540$ GeV exceeds $pp \to \gamma + X$ at $\sqrt{s} = 63$ GeV by two orders of magnitude, and $\bar{p}p \to \gamma + X$ at $\sqrt{s} = 63$ GeV by a factor of 60; with GHR it exceeds the former by a factor of 70 and the latter by a factor of 30.

On the other hand, at a fixed relatively low $p_T (\lesssim 10)$, our predicted collider ratios $(\gamma/\pi^0)_{\bar{p}p}$ are well below the corresponding ISR ratios. This is because at such p_T the π^0 cross sections increase even more. The reason is that at the corresponding collider x_T $(\lesssim 0.04)$ $\bar{p}p \to \pi^0 + X$ (and $\bar{p}p \to \text{jet} + X$) receives a strong contribution from the subprocess $gg \to gg$;[25,29] to $O(\alpha_s)$ there is no such contribution to $\bar{p}p \to \gamma + X$ (for the brems contribution of $gg \to gg\gamma$, see Fig. 3 and the next section).

Finally our predictions for $\bar{p}p \to \gamma + X$ at Tevatron energy ($\sqrt{s} = 1600$ GeV) are presented in Fig. 4 (some notation and scales as Fig. 3). Several of the remarks regarding collider predictions are the same, as, e.g., regarding the relative magnitude of the subprocesses (2.1) and (2.2). Notice that again the CDHS and GHR predictions differ little at the lower p_T, and this gives some confidence in our predictions although the corresponding x_T are very low. Since at such energies there is no experimental information on $\bar{p}p \to \pi^0 + X$, we prefer to present no predictions on the ratio γ/π^0.

We conclude this section with a few remarks on the uncertainties in our calculations. As we stated, the difference between CDHS- and GHR-based results gives a measure of the uncertainties in the parton (particularly gluon) distribution. Regarding the choice of Q^2, we have also carried calculations with $Q^2 = p_T^2$; the predicted total $E\,d\sigma/d^3p$ increase by a factor $\lesssim 1.5$. Changing the scale Λ in $\alpha_s(Q^2)$ from $\Lambda = 0.2$ to $\Lambda = 0.5$ GeV enhances the total $E\,d\sigma/d^3p$ by a factor ~ 1.35. The higher-order corrections (K factors) are positive and fairly large, as in Drell-Yan dilepton production and in other large transfer

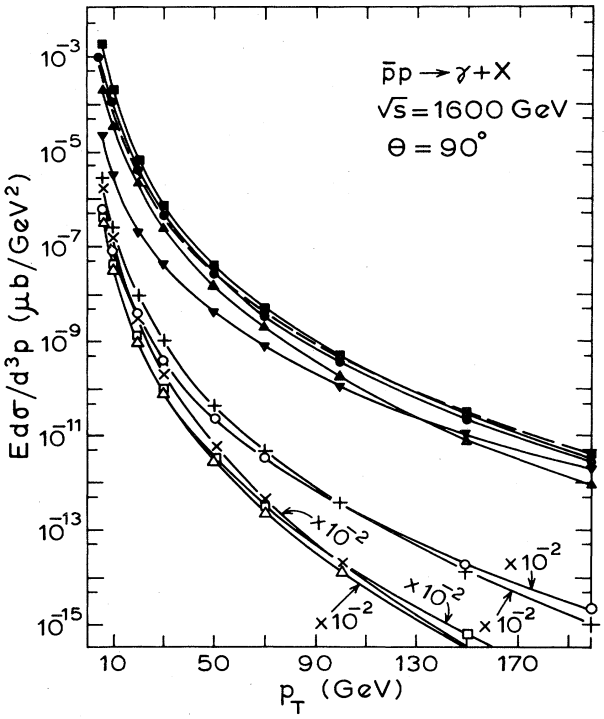

FIG. 4. $\bar{p}p \to \gamma + X$ at $\sqrt{s} = 1600$ GeV. Solid and dashed curves as in Fig. 1, but with multiplication factors as indicated (same as Fig. 3).

processes.[20,22] However, their magnitude is comparable to that of various uncertainties. For example, in all Figs. 1—4, at relatively large x_T the effect of the K factors is roughly the same as replacing the CDHS by the GHR set.

We have not considered higher-twist contributions. These may be important near kinematic end points.[4] Since we are restricted to $\theta = 90°$ we do not anticipate appreciable effects.

VI. BREMS CONTRIBUTIONS: ACCOMPANIED VS UNACCOMPANIED PHOTONS

We now discuss in some detail the brems contributions; the reasons for particular interest were stated in the Introduction.

For the physical process $AB \to \gamma + X$ consider the Born term of the brems contribution given by Eq. (2.10). The sum of such contributions are denoted by $E\,d\sigma_0(AB;\text{brems})/d^3p$. Consider also the Born contributions from the $O(\alpha_s)$ subprocesses Eqs. (2.1) and (2.2), given by Eq. (2.5); the sum of them is denoted by $E\,d\sigma_0(AB;\alpha_s)/d^3p$. We shall introduce the ratio

$$R(AB) \equiv \frac{E\,d\sigma_0(AB;\text{brems})/d^3p}{E\,d\sigma_0(AB;\alpha_s)/d^3p} . \tag{6.1}$$

According to the Introduction this should give a reasonable measure of the ratio of accompanied vs unaccompanied events. Of course, we can also introduce K factors and construct the corrected cross sections $E\,d\sigma(AB;\text{brems})/d^3p$ and $E\,d\sigma(AB;\alpha_s)/d^3p$. However, with our simple K factors [Eqs. (4.1), (4.2), and Ref. 25] we find that the resulting R differs little from Eq. (6.1). Then, in view of the involved approximations, it is sufficient to proceed with Eq. (6.1).

The magnitude of the brems contributions (and of R) depends rather significantly on the exact form of the fragmentation functions, i.e., of $d_{\gamma/q}(z)$ [and to a lesser extent on $d_{\gamma/g}(z)$]. The detailed brems contributions of Figs. 1—4 are calculated with the forms of Ref. 18 [Eqs. (2.15)—(2.18)] and with the CDHS set. However, below we present certain results corresponding to the forms (2.13) and (2.14) as well.

As a general remark, in all Figs. 1—4 the most important brems contribution arises from $qg \to qg\gamma$ (with $q \to \gamma$) for most of the x_T range considered. Next in importance is $qq \to qq\gamma$, which eventually (as x_T increases) dominates (see in particular Fig. 4, $\sqrt{s} = 1600$ GeV). These features are easily understood in terms of the dominance of $F_{g/p}$ at low x. The contribution from $gg \to q\bar{q}\gamma$ is way below; the reason lies in the form of the cross section and the color factor of $gg \to q\bar{q}$.[19] The contributions from $g \to \gamma$ fragmentation are understandably low. An exception is $gg \to gg\gamma$ at low p_T at the collider and Tevatron, which competes with $qq \to qq\gamma$. This is due to the importance of the subprocess $gg \to gg$ at the low collider and Tevatron p_T's (very low x_T.)[25,29,31]

We now turn to the ratios $R(AB)$, Figs. 5—7. All presented ratios correspond to the CDHS set except for the long-dashed curve which corresponds to GHR [with $d_{\gamma/q}(z)$ of Eq. (2.15)]. The highest (dash-dotted) curve in Figs. 5 and 6 corresponds to $d_{\gamma/q}(z)$ of Eq. (2.13), and the lowest (short-dashed) curve in all Figs. 5—7 to Eq. (2.14).

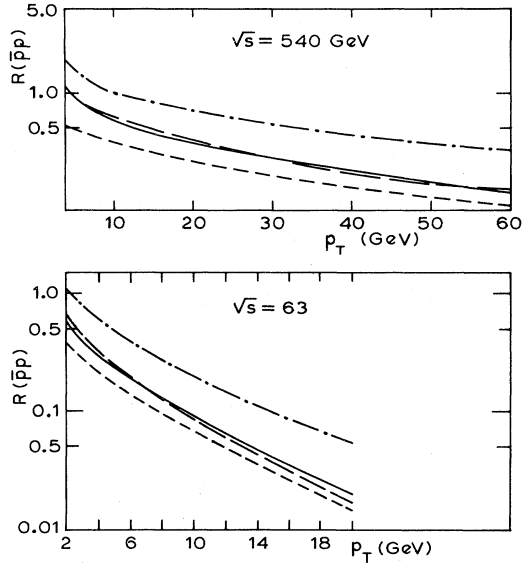

FIG. 5. Ratios $R(\bar{p}p) = E\,d\sigma_0(\bar{p}p;\text{brems})/d^3p / E\,d\sigma_0(\bar{p}p;\alpha_s)/d^3p$, which approximately correspond to events of photons accompanied vs unaccompanied by hadrons (see text). Solid curves: using $d_{\gamma/q}(z)$ of Eq. (2.15) and the CDHS set, long dashed curves: same $d_{\gamma/q}(z)$ and the GHR set; short dashed curves: using $d_{\gamma/q}(z)$ of Eq. (2.14) and CDHS; dash-dotted curves: $d_{\gamma/q}(z)$ of Eq. (2.13) and CDHS. Upper part: collider energy. Lower part: ISR.

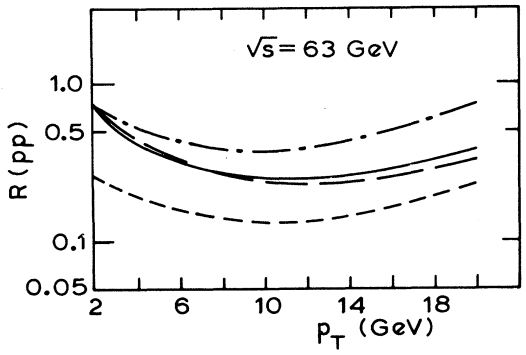

FIG. 6. Ratios $R(pp)=E\,d\sigma_0(pp;\ \text{brems})/d^3p/E\,d\sigma_0(pp;\ \alpha_s)/d^3p$ at ISR. Physical meaning and lines as in Fig. 5.

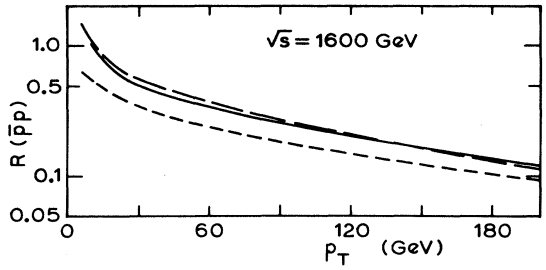

FIG. 7. Ratios $R(\bar{p}p)=E\,d\sigma_0(\bar{p}p;\ \text{brems})/d^3p/E\,d\sigma_0(\bar{p}p;\ \alpha_s)/d^3p$ at $\sqrt{s}=1600$ GeV. Physical meaning and lines as in Fig. 5.

The solid curve corresponds to Eq. (2.15); here for reasons of comparison we have neglected the (generally small) contributions corresponding to $g\to\gamma$ fragmentation.

The first remark is that in all Figs. 5—7 the two sets of distributions (CDHS and GHR) lead to very similar $R(AB)$, when, of course, the same $d_{\gamma/q}(z)$ is used. This is gratifying, for it indicates a stability against the various uncertainties.

We see that $R(\bar{p}p)$ at the collider (Fig. 5, upper part) and Tevatron (Fig. 7) is sizable ($>20\%$ for $p_T\lesssim 30$ GeV at the collider and $p_T\lesssim 80$ GeV at Tevatron). In particular, at collider $p_T\lesssim 10$ GeV and Tevatron $p_T\lesssim 20$ GeV, $R(\bar{p}p)\sim 1$; however, in this very low-x_T range our theoretical reservations should be kept in mind.

At $\sqrt{s}=63$ GeV $R(\bar{p}p)$ is sizable only at low $p_T(\lesssim 6$ GeV), and it decreases fast with p_T. In general, this decrease is due to the presence of the fragmentation function.

Note that $R(pp)$ at ISR is non-negligible throughout the entire p_T range. In particular, note the difference in p_T dependence between $R(\bar{p}p)$ and $R(pp)$. This can be understood in terms of the completely different role of the subprocess $q\bar{q}\to g\gamma$ in $pp\to\gamma+X$ vs $\bar{p}p\to\gamma+X$. In the former, this subprocess is of minor importance for all p_T (Fig. 1); in the latter it dominates all contributions for $p_T\gtrsim 7$ GeV, and as we discussed in Sec. V, it significantly enhances the cross section of $\bar{p}p\to\gamma+X$ relative to $pp\to\gamma+X$. As a result, $R(\bar{p}p)$ is a monotonically decreasing function of p_T.

The fact that $R(pp)$ at ISR shows some increase for $p_T\gtrsim 10$ GeV is understood from the fact that at such p_T the ratio of the contribution of $qq\to qq\gamma$ to that of $qg\to q\gamma$ increases with p_T (Fig. 1, open circles vs up-pointing triangles). This is because $qq\to qq\gamma$ involves valence quarks; and the importance of $F_{q/p}(x,Q^2)$ relative to $F_{g/p}(x,Q^2)$ increases with x (i.e., with x_T).

In Figs. 5 and 6 we also show $R(AB)$ calculated with $d_{\gamma/q}(z)$ of Eq. (2.13); this gives the largest $R(AB)$, in particular at the larger p_T. The same is true for $\sqrt{s}=1600$ GeV (not shown in Fig. 7). The reason is that this $d_{\gamma/q}(z)$ decreases slowly with z, and as $z\to 1$ tends to a constant limit ($=1$). The resulting $R(\bar{p}p)$ exceed by factors of 2 or more the ratios obtained with Eqs. (2.15) and (2.14). Note that Ref. 32 has obtained brems contributions exceeding those of the basic QCD subprocesses [Eqs. (2.1) and (2.2)]; the reason is essentially that they used $d_{\gamma/q}(z)$ of Eq. (2.13). There are, however, theoretical reasons for $d_{\gamma/q}(z)$ dropping rather fast with z and, in fact, for vanishing at $z=1$.[17,18] Thus we believe that Eq. (2.13) overestimates the brems contributions. In this we are in accord with Ref. 14.

Noted added in proof. After the completion of this work we received a report [E. Berger, E. Braaten, and R. Field, Florida Report No. UFTP-83-20 (unpublished)], which in part deals with the same subject. Although its input parton distributions are different, the results are very similar to ours.

ACKNOWLEDGMENTS

We would like to thank R. Horgan and M. Jacob for useful discussions, suggestions, and critical remarks, and V. Cavasinni, C. Leroy, and J. Trischuk for useful and stimulating discussions. One of us (A.P.C.) would like to thank the Theoretical Study Division of CERN for its hospitality during a visit when part of this work was done. This work was supported in part by the Natural Sciences and Engineering Research Council of Canada and by the Quebec Department of Education.

[1]W. Willis, in *Proceedings of the 4th International Colloquium on Photon-Photon Interactions, Paris, 1981,* edited by Georges W. London (World Scientific, Singapore, 1981); Report No. CERN-EP/81-45 (unpublished); I. Manneli, in *Proceedings of the 1981 International Symposium on Lepton and Photon Interactions at High Energies, Bonn,* edited by W. Pfeil (Physikalisches Institut, Universität Bonn, Bonn, 1981); L. Resvanis, in the *Multiparticle Dynamics, 1981,* proceedings of the XII International Symposium, Notre Dame, Indiana, edited by W. D. Shepard and V. P. Kenney (World Scientific, Singapore, 1982).

[2]A. Angelis *et al.*, Phys. Lett. 94B, 106 (1980); M. Tannenbaum, in *Particles and Fields—1979,* proceedings of the Annual Meeting of the Division of Particles and Fields of APS, Montreal, edited by B. Margolis and D. G. Stairs (AIP, New York 1980); E. Amaldi *et al.*, Nucl. Phys. B150, 326 (1979).

[3]M. McLaughlin *et al.*, Phys. Rev. Lett. 51, 971 (1983); B. Cox, in *Proceedings of the 1979 International Symposium on Lep-*

ton and Photon Interactions at High Energies, Fermilab, edited by T. B. W. Kirk and H. D. I. Abarbanel (Fermilab, Batavia, Illinois, 1980).

[4]T. Ferbel and W. Molzon, Rev. Mod. Phys. (to be published).

[5]V. Cavasinni *et al.*, proposal submitted to CERN, 1983 (unpublished).

[6]We thank M. Albrow and M. Jacob for informative discussions.

[7]H. Abramowicz *et al.*, Z. Phys. C 12, 289 (1982); 17, 283 (1983); K. Kleinknecht (private communication) [CERN-Dortmund-Heidelberg-Saclay (CDHS) Collaboration].

[8]M. Glück, E. Hoffmann, and E. Reya, Z. Phys. C 13, 119 (1982).

[9]P. Aurenche and J. Lindfors, Nucl. Phys. B168, 296 (1980).

[10]A. P. Contogouris, S. Papadopoulos, and C. Papavassiliou, Nucl. Phys. B179, 461 (1981); and with E. Argyres, in *Proceedings of the XIth International Symposium on Multiparticle Dynamics, Bruges, Belgium, 1980,* edited by E. DeWolf and F. Verbeure (University of Antwerp, Antwerp, Belgium, 1980).

[11]J. Kripfganz *et al.*, in *Proceedings of the XVth Rencontre de Moriond,* edited by J. Tran Thanh Van (Editions Frontieres, Dreux, France, 1980); A. P. Contogouris, in *High Energy Physics—1980,* proceedings of the XXth International Conference, Madison, Wisconsin, edited by L. Durand and L. G. Pondrom (AIP, New York, 1981).

[12]M. Dechantsreiter, F. Halzen, and D. Scott, Phys. Rev. D 24, 2856 (1981); D. Scott, in *Proceedings of the 21st International Conference on High Energy Physics, Paris, 1982,* edited by P. Petiau and M. Porneuf [J. Phys. (Paris) Colloq. 43 (1982)].

[13]M. Nowak and M. Praszalowicz, Z. Phys. C 17, 249 (1983).

[14]O. Benary, E. Gotsman, and D. Lissauer, *ibid.* 16, 211 (1983).

[15]F. Halzen and D. Scott, Phys. Rev. Lett. 40, 1117 (1978); Phys. Rev. D 18, 3378 (1978).

[16]A. P. Contogouris, S. Papadopoulos, and M. Hongoh, Phys. Rev. D 19, 2607 (1979).

[17]W. Frazer and J. Gunion, Phys. Rev. D 20, 147 (1979), and references therein. For more recent developments see, e.g., M. Glück, in *Proceedings of the International Europhysics Conference on High Energy Physics, Brighton, 1983,* edited by J. Guy and C. Costain (Rutherford Appleton Laboratory, Chitton, Didcot, 1984).

[18]A. Nicolaidis, Nucl. Phys. B163, 156 (1980).

[19]B. Combridge, J. Kripfganz, and J. Ranft, Phys. Lett. B70, 234 (1977); R. Cutler and D. Sivers, Phys. Rev. D 17, 196 (1978).

[20]A. P. Contogouris, S. Papadopoulos, and J. Ralston, Phys. Rev. D 25, 1280 (1982); Phys. Lett. 104B, 70 (1981). (a) Very recently a complete calculation has appeared [P. Aurenche *et al.*, Annecy Report No. LAPP-TH-96 (unpublished)]. For conventional choices of the large variable, e.g., $Q^2=p_T^2$, the resulting $O(\alpha_s^2)$ corrections are similar to ours [Eqs. (4.1) and (4.2)] at both CERN collider and ISR energies (only a bit bigger). Those authors consider also an unconventional choice. Then the $O(\alpha_s^2)$ corrections are different, but the resulting corrected cross sections differ less then ours when we replace the GHR set by the CDHS set. The overall conclusion is that, with conventional choices of Q^2 ($=p_T^2$ or $2p_T^2$), our K factors give a very reasonable estimate of the $O(\alpha_s^2)$ corrections.

[21]M. Krawczyk, Warsaw Report No. IFT/2/83 (unpublished); A. Czechowski and M. Krawczyk, Z. Phys. C 19, 95 (1983).

[22]A. P. Contogouris, Phys. Rev. D 26, 1618 (1982).

[23]R. Ellis, G. Martinelli, and R. Petronzio, Nucl. Phys. B211, 106 (1983); H. Perlt, Z. Phys. C 17, 153 (1983).

[24]It is quite possible that near the kinematic end point ($x_T\sim 0$ or $x_T\sim 1$) the $O(\alpha_s^2)$ corrections from a complete calculation significantly differ from the K factors of Eqs. (4.1) and (4.2). The same may hold for the corrections to the subprocesses $ab\rightarrow cd$.[25] Notice, however, that the K factors of Ref. 25 lead to predictions in good agreement with collider (and ISR data on large-p_T pion production down to $x_T\simeq 7.5\times 10^{-3}$.

[25]N. Antoniou *et al.*, Phys. Lett. 128B, 257 (1983); Phys. Rev. D 29, 1354 (1984).

[26]E. Anassontzis *et al.*, Z. Phys. C 13, 277 (1982) (Athens-Brookhaven-CERN Collaboration).

[27]T. Akesson *et al.*, Phys. Lett. 121B, 439 (1983); Nucl. Phys. B228, 409 (1983) (Axial Field Spectrometer Collaboration).

[28]M. Banner *et al.*, Phys. Lett. 115B, 59 (1982) (UA2 Collaboration).

[29]R. Horgan and M. Jacob, Nucl. Phys. B179, 441 (1981).

[30]P. Bagnaia *et al.*, Z. Phys. C 20, 117 (1983) (UA2 Collaboration).

[31]P. Darriulat, concluding talk, in *Moriond Workshop on $\bar{p}p$ Physics and the W Discovery, La Plagne-Savoie, 1983,* edited by J. Tran Thanh Van (Editions Frontieres, Dreux, France, 1983), p. 635.

[32]R. Horgan and P. Scharbach, Nucl. Phys. B181, 421 (1981).